Two-Dimensionally Self-Arranged Protein Nanoarrays on Diblock Copolymer Templates

Nitin Kumar, Omkar Parajuli, and Jong-in Hahm*

Department of Chemical Engineering, The Pennsylvania State University, 160 Fenske Laboratory, University Park, Pennsylvania 16802

Received: December 11, 2006; In Final Form: March 2, 2007

Novel methods for creating protein arrays with two-dimensional control can significantly enhance basic biological research as well as various bioarray applications. We demonstrate that the structural variety and chemical heterogeneity of self-assembled, hexagonal polystyrene-*b*-poly(vinylpyridine) micelles can be successfully exploited as templates for easy and rapid fabrication of functional protein arrays over a large scale. Spontaneous formation of such polymeric template-guided protein molecules yields high-density protein arrays that exhibit repeat spacings in a nanoscopic dimension. The ensuing self-assembled protein molecules in the array maintain their natural conformation and activity over a very long time period. By tuning the size of the underlying block copolymer templates, our amphiphilic diblock copolymer-based approach to create high-density protein patterns also permits spatial control over two-dimensional repeat spacings of protein nanoarrays. These unique advantages of polystyrene-*b*-poly(vinylpyridine) templates make the spontaneously constructed protein nanoarrays highly suitable as functional protein sensor substrates. Therefore, our novel two-dimensional protein assembly method can be greatly beneficial for high-throughput proteomic assays and multiplexed high-density protein sensing applications.

Protein arrays are utilized as active supports for a variety of diagnostic assays in tissue engineering, pharmacology, and proteomics.[1−14] High-density protein arrays, consisting of active and surface-immobilized protein molecules in a periodic manner, can greatly benefit these applications. Ideal protein sensors should be capable of delivering efficient, sensitive, parallel, and automated analyses that can be applied to large numbers of samples with greatly reduced volume of sample and reagent usage.[2,3,7,11,15] Such biosensor platforms can, in turn, facilitate rapid, high-throughput screening and immunoassays by enabling an escalated degree of miniaturization in surface-based biotechnologies. Successful development of these protein arrays would require a straightforward method to immobilize proteins on a solid surface with a precise and nanoscale spatial control. However, inherent difficulties associated with positioning these small protein molecules have restricted to date both the study and application of nanoscaled protein arrays. To this end, reliable placement of protein molecules in well-defined nanoscale patterns while retaining their native functionality is essential for overcoming the current limitations of protein arrays. Thus, a novel method that can conveniently and rapidly organize proteins into high-density arrays with nanoscale resolution is highly warranted.

A variety of methods for protein localization have been previously explored. Surface deposition techniques for proteins include ink-jet and pipette deposition,[7,16,17] soft lithography,[18−20] dip-pen lithography and related scanning probe patterning methods,[21−24] focused-ion-beam patterning,[25] imprint lithography,[26] and microfluidic channel networks.[27−29] As a step forward toward overcoming limitations associated with these techniques such as low protein address density and slow assembly speed, we have previously developed nanoscale protein arrays by exploiting the self-organizing nature of polystyrene-*block*-poly(methyl methacrylate) (PS-*b*-PMMA) diblock copolymer templates and the self-segregating tendency of proteins to preferential PS domains.[30] In this previous work, nanometer-scale, surface-bound protein patterns were instantly achieved via self-assembly where nanoscale spatial control of proteins was achieved without undergoing a series of time-consuming fabrication or modification processes. This previous study exploited a self-assembly property of half cylinder-forming block copolymer, namely, that these systems create arrays of parallel lines with a controllable repeat spacing in the direction perpendicular to the lines. However, to create protein arrays widely applicable in basic biological research and biotechnology, control over additional degrees of freedom in the spatial arrangement of proteins on the nanometer scale, that is, two-dimensionally controlled periodicity, is highly warranted.

In this paper, we turn to the rich morphology of amphiphilic diblock copolymers to achieve rapid, large-area self-assembly of two-dimensionally controlled protein arrays with a periodic repeat spacing in nanoscopic dimensions. Micellar assembly of amphiphilic diblock copolymers above a critical polymer concentration is a well-known behavior. Amphiphilic polymeric systems such as polystyrene-*b*-poly(acrylic acid), poly(ethylene propylene)-*b*-poly(ethylene oxide), polystyrene-*b*-poly(2-vinylpyridine), and polystyrene-*b*-poly(4-vinylpyridine) were extensively studied to understand their fascinating micellar properties and dependence on diblock copolymer characteristics.[31−34] The exact structures and configurations of the resulting micelles or aggregates are determined by the composition of the diblock polymer, the length of each polymer segment, the polarity of the solvent, and the relative solubility of each polymer block in the solvent. Although the nanoscale micellar templates of diblock copolymer films have been used as seed sites for inorganic nanoparticle or nanowire growth as well as nanocarriers for drug molecules in the past,[35−44] their applications as nanoscale arrayed biotemplates have never been demonstrated

* To whom correspondence should be addressed. E-mail: jhahm@engr.psu.edu.

10.1021/jp068509p CCC: $37.00
Published on Web 04/11/2007

before. Yet, these amphiphilic diblock copolymers can serve as extremely useful guides in organizing biomolecules into two-dimensional arrays since they exhibit a rich spectrum of morphologies and their repeat spacings are tunable in two dimensions.

Herein, we demonstrate that polystyrene-*b*-poly(4-vinylpyridine) (PS-*b*-PVP) can be effectively used for the self-assembly of surface-bound, two-dimensional nanoscale protein arrays where the periodicity of repeating protein patterns can be effectively controlled by the nearest-neighbor spacing in the underlying hexagonal array. We also establish a straightforward method to produce protein patterns of different geometries and sizes by successfully manipulating topological structures of underlying PS-*b*-PVP templates. Further, we report our findings on the activity and stability of various model proteins on these PS-*b*-PVP templates. The model proteins chosen in our study include bovine immunoglobulin G (IgG), mushroom tyrosinase (MT), and horseradish peroxidase (HRP). These proteins are commonly used not only in biological research but also in biomedical applications where their flexibility of usage can range widely from purifying antibody molecules, to detecting antigen−antibody complexes, and to investigating enzymatic activity. Our polymer-guided self-assembly approach enables facile, two-dimensional control of nanoscale protein patterns. Equally important, our new approach leads to protein arrays that maintain their biological activity and specific functionality over a long period of time. Such advantages of our polymer-based method are crucial in creating much needed, high-density, functional protein arrays which, in turn, can be extremely beneficial for improved basic biological assays and high-throughput biomedical tests.

To demonstrate that diverse surface PS-*b*-PVP geometries can be easily self-assembled on the nanoscopic scale and subsequently empolyed to construct nanoscale protein arrays with spatial control in two dimensions, we first describe the simple and robust methods which we used to create an assortment of PS-*b*-PVP micellar templates. Asymmetric PS-*b*-PVP diblock copolymer with an average molecular weight of 68 500 Da was obtained from Polymer Source Inc. (Montreal, Canada). The diblock contained 70% of PS by weight with a polydispersity of 1.14. The protein assembly demonstrated in this paper utilizes the three PS-*b*-PVP micellar thin film templates, illustrated schematically in Figure 1. We categorize the two-dimensionally periodic nanoscale PS-*b*-PVP templates as (i) original, (ii) open, and (iii) reverted PS-*b*-PVP micelles.

Upon dissolution of 0.5% (w/v) PS-*b*-PVP in toluene, micelles consisting of a PVP core and a PS corona readily formed, as toluene is a preferential solvent for PS. This micellar solution was then spun on silicon substrates at 3500 rpm for 1 min. Silicon substrates, obtained from Silicon Inc. (Boise, Idaho), were cleaned with ethanol, acetone, and toluene and spun dry before coating ultrathin PS-*b*-PVP films. Atomic force microscopy (AFM) measurements were carried out using Digital Instruments Multimode Nanoscope IIIa in tapping mode at a scan speed of 1 Hz. Silicon tips with a resonant frequency of 60 kHz and a spring constant of 5 N/m were used in our measurements.

Figure 2A displays topographic AFM images of these PS-*b*-PVP micelles on a silicon substrate. The topographical AFM images clearly show a two-dimensional array of PS-*b*-PVP micelles that are hexagonally packed. We refer to these spherical PS-*b*-PVP micelles as "original" PS-*b*-PVP templates. Individual micelles in the original template are approximately 50 nm in diameter. The height difference between the lower region

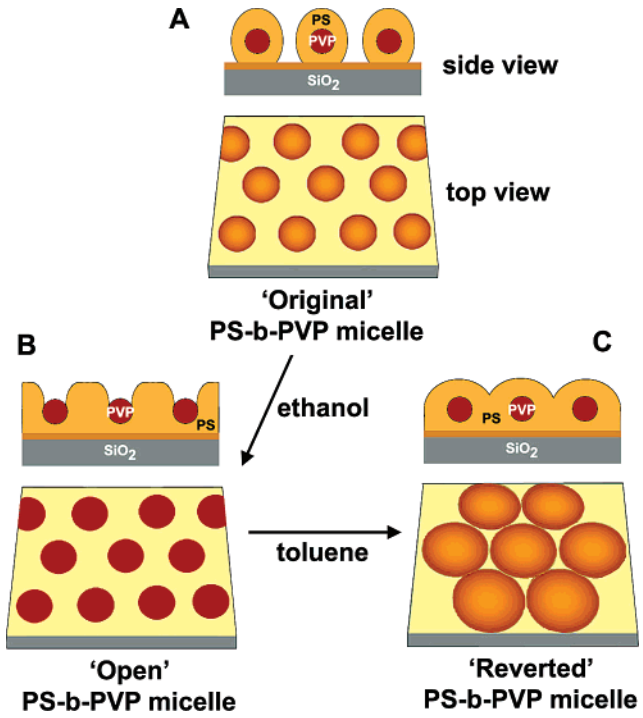

Figure 1. Schematic cartoons illustrating the top and side views of various polymeric templates: (A) original, (B) partially open, and (C) reverted two-dimensional PS-*b*-PVP micelles on silicon substrates. These templates were subsequently used for nanoscale self-assembly of two-dimensional protein arrays.

surrounding the micelles and the top of the micelles is measured as ∼7−8 nm. The core and corona of these micelles can be partially opened by exposing the original PS-*b*-PVP templates on silicon substrates to a solvent favoring PVP such as ethanol.[45] Micelles with partially open PS coronae exposing their PVP cores were produced by introducing an ethanol vapor to the original template for 15 min. The resulting '"open" PS-*b*-PVP templates are shown in the topographic AFM images in Figure 2B. The elevations in Figure 2A turned into depressions in Figure 2B as the exposure of the original PS-*b*-PVP template to ethanol vapor leads to rearrangements of the PS chains at the air/polymer interface, partially uncovering the core PVP chains of the original micelles, as illustrated in Figure 1B. The array of PVP depressions that are surrounded by taller PS chains persisted over a large area of the substrate. Each hole, seen as dark depression spots in Figure 2B, in the hexagonally packed open PS-*b*-PVP template measures approximately 37 nm in diameter and ∼8−9 nm in depth. Upon further treatment of the open PS-*b*-PVP micelles with a toluene vapor for 15 s, these open templates were switched to yet another type of micellar morphology shown in the topographic AFM images of Figure 2C. The hexagonally packed micelles in the resulting '"reverted" PS-*b*-PVP template resemble the original template. To minimize the unfavorable interaction between PVP and toluene, the partially exposed PVP cores are recovered by PS in the reverted template. However, the micelles in the reverted PS-*b*-PVP are larger in width and shorter in height than the original micelle, where individual micelles in the reverted template measure approximately 60 nm in diameter and ∼3−4 nm in height. The center of the reverted micelle is slightly lower in height than its surrounding, as shown in the height profile along a reverted micelle in Figure 2C. This observation may possibly be explained by incomplete refolding of PS chains to enclose the PVP core.

Whole molecule bovine IgG was purchased from VWR

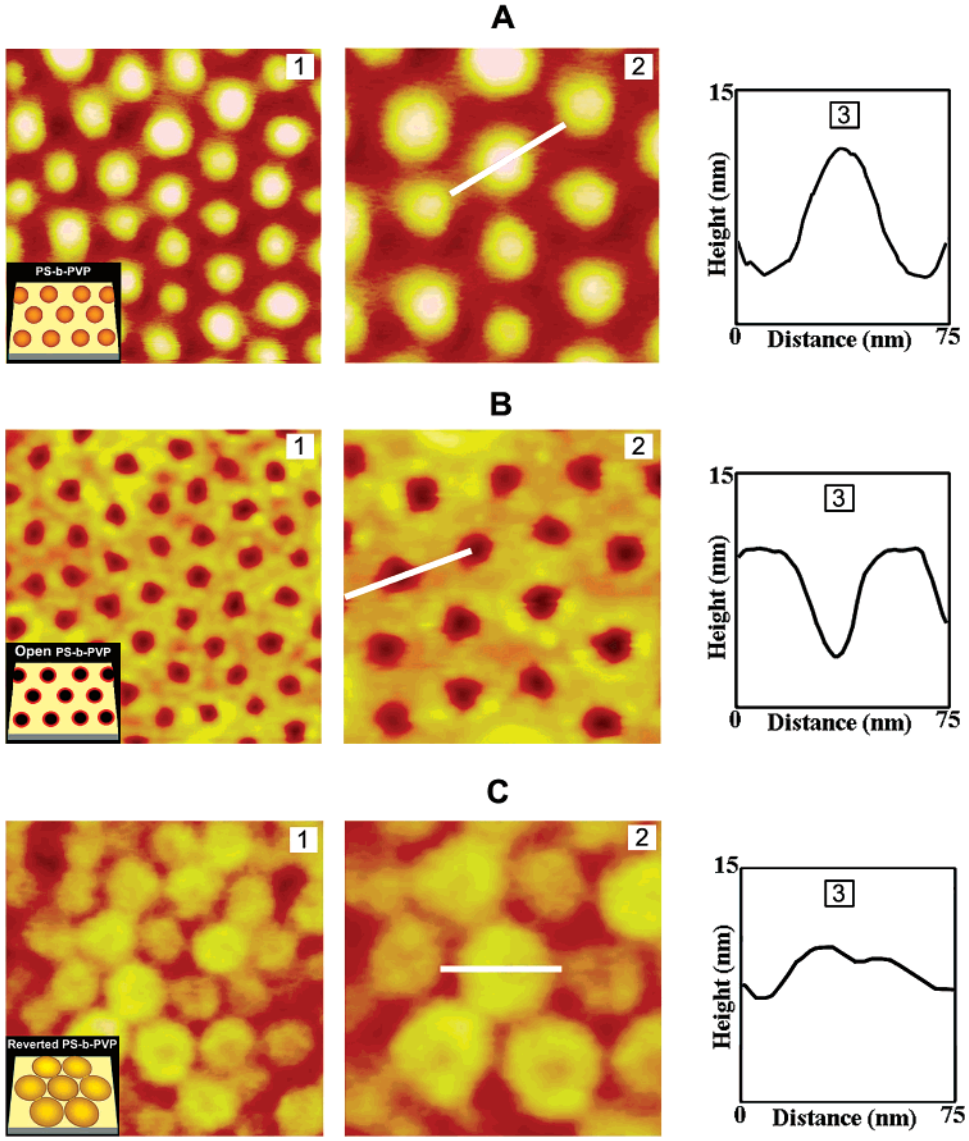

Figure 2. AFM topology of various self-assembled nanoscale PS-*b*-PVP templates prepared by various solvent exposures. (A) (1 and 2) 300 × 300 and 180 × 180 nm AFM images showing the '"original" hexagonally packed PS-*b*-PVP micellar film that was spun cast in toluene on a silicon substrate. (3) Height profile along the indicated white line of the original micelle shown in (2). (B) (1 and 2) 300 × 300 and 180 × 180 nm AFM images displaying surface morphology changes of the original PS-*b*-PVP templates into open micelles due to ethanol exposure. (3) Height profile measured along the open micelle as indicated with the inserted white line in (2). PS chains of the original micelle at the polymer/air interface spread open away from the micelle center and exposing the low-lying PVP core shown as darker circles in the AFM images. (C) (1 and 2) 300 × 300 and 180 × 180 nm AFM images revealing reverted micellar templates upon further toluene vapor treatment of samples shown in B. (3) Topographical profile analyzed along the inserted line on the reverted micelle in (2). Hexagonally packed nanoscale micelles resembling the original PS-*b*-PVP templates were formed spontaneously over a large area.

Scientific Inc. (West Chester, PA), and mushroom tyrosinase was obtained from Sigma-Aldrich (St. Louis, MO). Lyophilized powder of these protein molecules were reconstituted in a PBS buffer (10 mM mixture of Na_2HPO_4 and NaH_2PO_4, 140 mM NaCl, 3 mM KCl, pH 7.4) to varying concentrations. A total of 100 μL of desired protein solution was then deposited onto the ultrathin PS-*b*-PVP micelle films for 20 s at room temperature. The sample surface was then thoroughly rinsed with PBS buffer followed by gentle blow-drying under a stream of nitrogen gas. AFM data shown in Figure 3 correspond to typical topography images of (A and B) IgG and (C) MT deposited on various PS-*b*-PVP templates. Figure 3A clearly demonstrates that IgG molecules adsorb preferentially on the PS-rich regions of the open PS-*b*-PVP template when a 20 μg/mL solution of IgG molecules is deposited on the PS-*b*-PVP template as shown in Figure 2B. As PS chains occupy the neighboring regions between holes in the open PS-*b*-PVP template, individual IgG molecules assemble in the perimeter areas of holes as seen in the zoomed-in image of Figure 3A-4. Since PS regions of the reverted PS-*b*-PVP space-fill around the hexagonally arrayed PVP cores, IgG molecules form structures surrounding the hexagonal spaces. Due to the adsorption of IgG molecules onto PS domains of the open template, the height difference between the center of the hole and the IgG-bound region is ~13−14 nm. Figure 3B displays AFM images of IgG molecules self-assembled on reverted PS-*b*-PVP templates. A single layer of IgG molecules cover PS-rich regions in the reverted templates at a concentration of 10 μg/mL where typically three IgG molecules assemble into close-packed structures on top of the refolded PS chains, as shown in the zoomed-in image of Figure 3B-4. The onset of the close-packing individual protein molecules on PS domains is seen on the sample prepared with 4 μg/mL protein concentration; see Figure 3B-2. AFM data in Figure 3C show self-assembly of MT molecules on the reverted

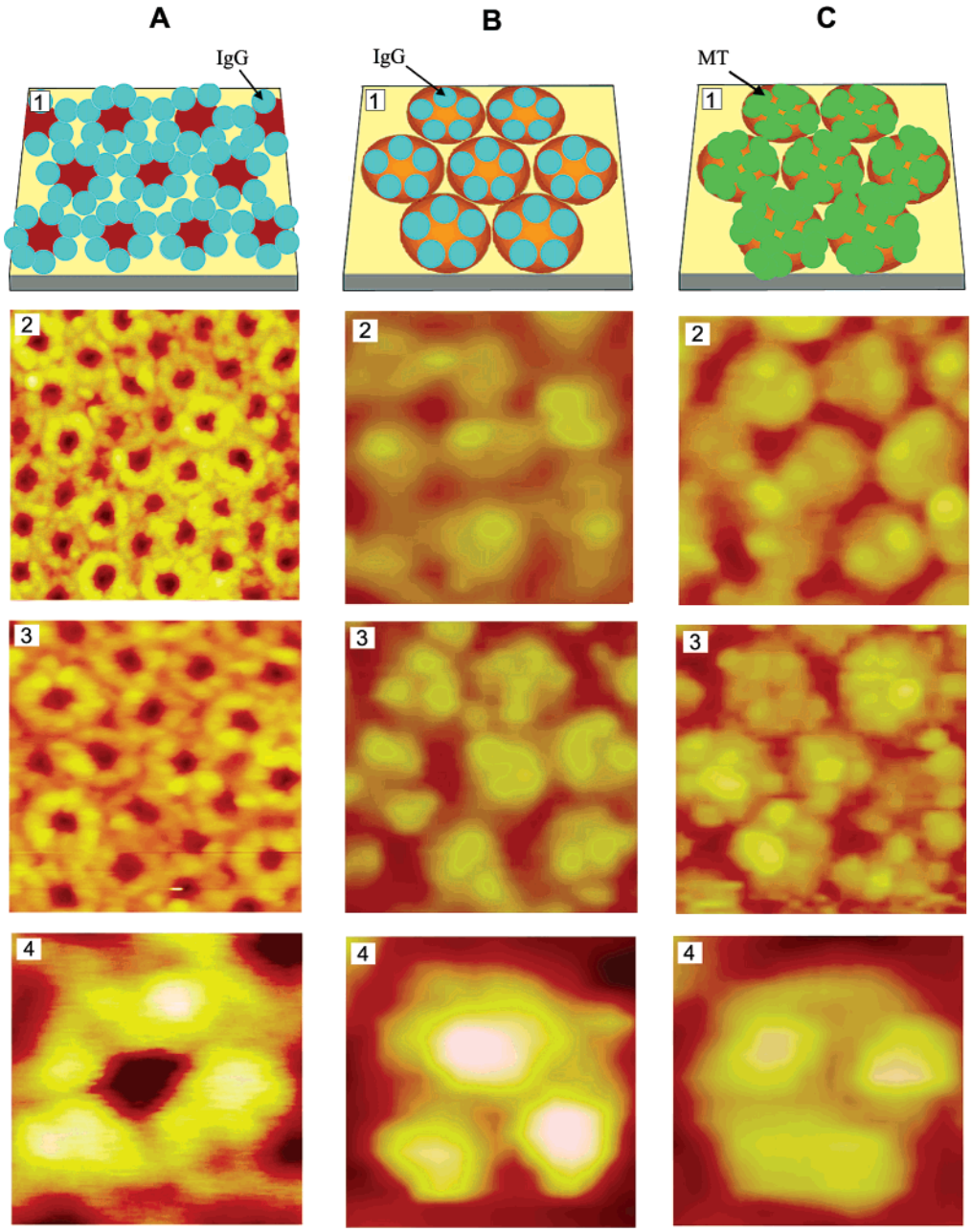

Figure 3. Schematic illustrations and AFM topography images of IgG and MT molecules on PS-*b*-PVP templates. (A) IgG molecules deposited on open PS-**b**-PVP templates from a 20 μg/mL solution. The presented AFM images are (2) 300 × 300 nm, (3) 180 × 180 nm, and (4) 60 × 60 nm in size. On open PS-*b*-PVP micellar templates, IgG molecules occupy preferentially the PS-rich areas which encircle the hexagonally packed, low-lying PVP cores. (B) IgG molecules assembled on reverted PS-*b*-PVP templates when (2) 4 μg/mL and (3 and 4) 10 μg/mL of IgG solution was added to the templates. (C) MT molecules assembled on reverted PS-*b*-PVP templates when (2) 4 μg/mL and (3 and 4) 20 μg/mL of MT solution was added to the templates. Individual protein molecules are visible on the micellar surface of the reverted PS-*b*-PVP templates in panels B and C at the 4 μg/mL concentration, whereas the compact packing nature of those individual protein molecules on the micelles due to increased protein concentration is clearly resolved in the AFM images of the 10 μg/mL IgG and 20 μg/mL MT samples. The scan size of the topographical AFM images shown in B and C corresponds to (2) 180 × 180 nm, (3) 180 × 180 nm, and (4) 60 × 60 nm.

PS-*b*-PVP templates. Similar to IgG molecules, they selectively segregate onto PS-rich areas of the underlying template. Individual protein molecules are clearly resolved on the micellar surface of the reverted PS-*b*-PVP templates in parts C-2 and C-3 of Figure 3 which were prepared at MT concentrations of 4 and 20 μg/mL, respectively. The compact packing nature of MT, arrangement of protein molecules on PS domains, and the number of protein molecules occupying the surface of a single micelle are very similar to that of IgG as they have comparable molecular weights.

For all protein molecules under investigation, AFM line measurements of the height difference between bare polymer templates and adsorbed proteins on these polymer templates yielded much lower values than expected from known diameters of these proteins. This effect is induced by AFM tip−sample interactions as compliant biological samples were probed intermittently under our tapping mode imaging conditions. Similar effects to our observed height reduction have been previously reported in tapping mode AFM imaging studies of soft biological molecules such as proteins and DNA.[46,47]

To assess biological activity of the two-dimensional protein nanoarrays prepared using PS-*b*-PVP templates, we carried out an enzymatic activity measurement of HRP molecules. HRP molecules were first immobilized on the original PS-*b*-PVP

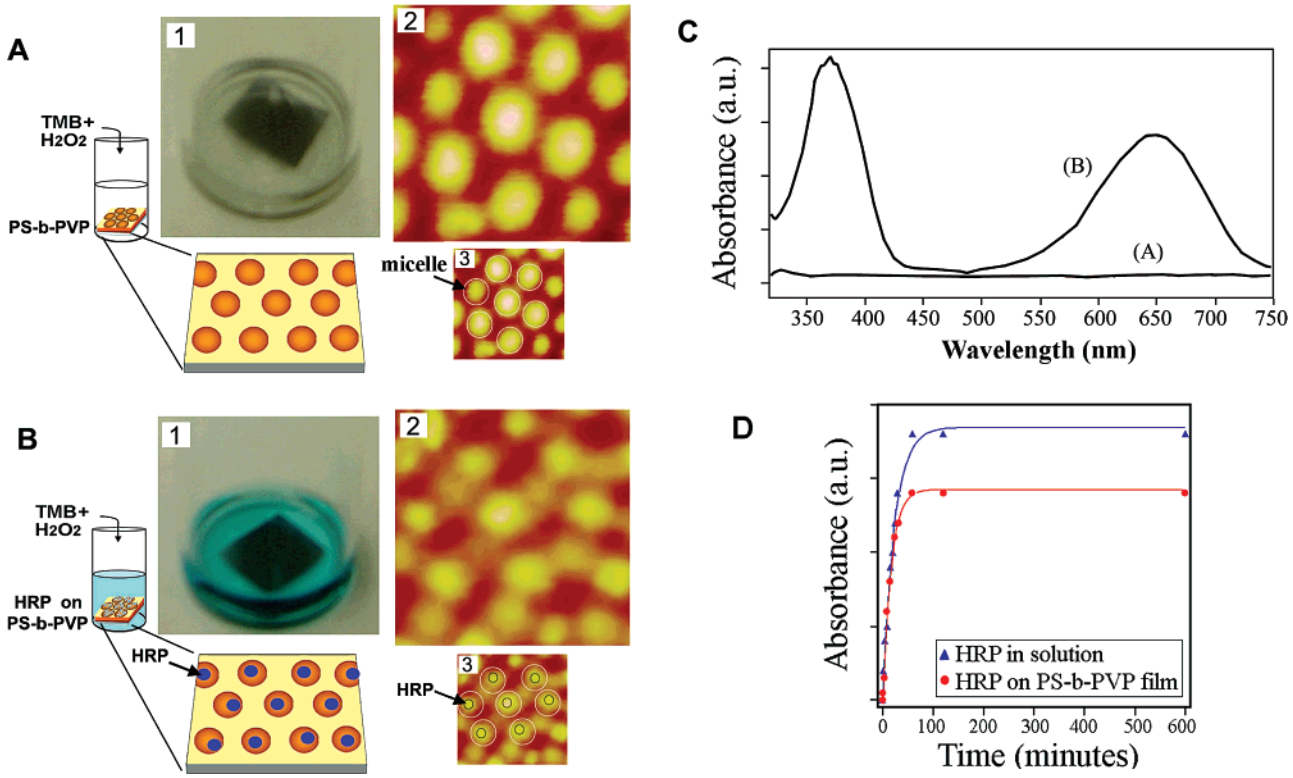

Figure 4. Enzymatic activity test of HRP adsorbed on PS-*b*-PVP ultrathin micellar films. (A) Control experiment without HRP molecules on PS-*b*-PVP. (1) In the absence of HRP, color change of the assay solution was not observed. (2) A 180 × 180 nm AFM image of the hexagonally packed PS-*b*-PVP micelles which was used in the enzymatic assay shown in (1). (3) Each PS-*b*-PVP micelle in the hexagonal lattice of the AFM image shown in (2) is circled for clarity. (B) Enzymatic activity experiment with 10 μg/mL HRP on PS-*b*-PVP. (1) Digital image of a TMB assay solution after addition to HRP-bound PS-*b*-PVP micelles on a silicon substrate. The assay color rapidly changed from colorless to blue. (2) 180 × 180 nm AFM image revealing the sample surface employed in the enzymatic test shown in (1). (3) To guide the eye, black and white circles are inserted in the AFM image shown in (2) to indicate the surface-bound HRP molecules and the underlying PS-*b*-PVP micelles, respectively. HRP molecules organize themselves on top of the underlying, hexagonally packed PS-*b*-PVP micelles which, in turn, form periodic, two-dimensional nanoscale protein arrays. (C) UV−vis absorbance spectra of the TMB assay solutions shown in A and B. (A) No absorbance peaks were observed when TMB solution containing hydrogen peroxide was introduced to a PS-*b*-PVP micellar thin film containing no HRP on its surface. (B) Characteristic UV−vis absorbance peaks were monitored from the blue assay solution. (D) UV−vis absorbance of HRP molecules monitored over time in solution (data shown in blue) and on PS-*b*-PVP micelles (data shown in red). When compared with the activity of HRP molecules in solution, HRP molecules bound on PS-*b*-PVP showed 78% of the activity measured in solution.

micellar template. The enzymatic activity of these surface-bound HRP molecules was subsequently monitored over a long period of time. HRP is a widely used, highly specific enzyme that catalyzes reduction of hydrogen peroxide at a high turnover rate in a short period of time.[48] HRP and 3,3′,5,5′-tetramethylbenzidine (TMB) solution containing 1.25 mM TMB and 2.21 mM H_2O_2 were purchased from VWR Scientific Inc. (West Chester, PA). The lyophilized powder of HRP was reconstituted in deionized water to a final concentration of 10 μg/mL. An amount of 100 μL of the enzyme solution was deposited onto the original PS-*b*-PVP templates for 20 s at room temperature. The sample surfaces were thoroughly rinsed with deionized water. Visualization of HRP activity was carried out in the presence of TMB. This chemical process transfers electrons from TMB to peroxidase, changing the solution color from colorless to blue. A digital camera, Sony Cybershot DSC-P92, was used to capture the assay color changes. UV−vis spectra were recorded on a Hewlett-Packard 8452A Diode Array spectrophotometer.

Figure 4 summarizes the results of our HRP activity test on original PS-*b*-PVP templates. When PS-*b*-PVP micellar templates were exposed to the TMB assay solution without any surface-bound HRP as a control, no color change was observed, as shown in Figure 4A-1. On the contrary, when the TMB assay solution was added to PS-*b*-PVP micellar templates containing HRP molecules, the color of the solution rapidly turned from colorless to blue; see Figure 4B-1. The density of the enzyme molecules bound on the original PS-*b*-PVP templates was ~3 × 10^{10} molecules/cm^2 when they were adsorbed from a 10 μg/mL HRP solution. The AFM images in parts A-2 and B-2 of Figure 4 clearly display the surface morphology of the micellar templates used in our activity test without and with HRP molecules, respectively. As shown in Figure 4B-2, HRP molecules organize themselves on top of the underlying, hexagonally packed PS-*b*-PVP micelles which, in turn, yields periodic, two-dimensional nanoscale protein arrays. HRP molecules occupying the top sites of the original PS-*b*-PVP micellar template are higher than the original micelles by ~2.5−3 nm. Figure 4C displays UV−vis spectra of the two assay solutions prepared for the HRP enzymatic activity test as shown in parts A-1 and B-1 of Figure 4; no absorption peaks were observed in the absence of HRP whereas, in the presence of HRP, characteristic absorption peaks corresponding to oxidized TMB were monitored. The enzyme molecules of HRP on PS-*b*-PVP templates remained active for reduction of hydrogen peroxide even after 100 days when kept at 4 °C.

We also monitored differences in HRP activity between free vs PS-*b*-PVP micelle-bound HRP molecules by performing time-dependent UV−vis measurements. Two samples containing comparable amounts of the enzyme molecules, approximately 7.5 × 10^9 molecules, were used for this comparison experiment. In one sample, HRP molecules were prepared in a solution whereas, in the other sample, the enzyme molecules were bound

on a PS-*b*-PVP template. UV−vis absorbance was then monitored over time, and the absorption maximum at 650 nm was recorded as a function of time; see Figure 4D. Data from the free HRP sample are shown in blue and those from the bound HRP on PS-*b*-PVP micelles are shown in red. When compared with the activity of unbound HRP molecules in solution, HRP molecules bound on PS-*b*-PVP retained 78% of the activity measured in solution. These results indicate that much of the enzyme molecules indeed maintain their natural conformation and activity when they are effectively immobilized on the underlying PS-*b*-PVP templates via self-assembly.

Our data also suggest that amphiphilic diblock copolymer templates permit control of the spatial resolution of adsorbed proteins on the nanometer scale by site-selective adsorption of proteins onto template surfaces displaying a spatially defined, chemical heterogeneity. When their rich, extensively characterized, and precisely controlled surface morphology is exploited, these polymeric surfaces can serve very efficiently as two-dimensional nanoscale guides for spontaneously constructed protein arrays that feature high areal density, stable protein conformation, and no loss of protein activity. We envision that immediate applications of our protein nanoarrays will involve the use of currently available microsample handling and detection apparatus, where a group of multiple micelles will serve as a single, independently addressable unit in a given protein array. However, ideal application of our protein nanoarrays would be able to address each micelle as an independent unit on the nanoscale where a single protein array would contain a large number of different proteins to be examined. Therefore, to take full advantage of our diblock copolymer-based nanoscale protein arrays, conventionally available methods of sample delivery as well as detection systems need to be improved to provide a nanoscopic spatial resolution.

In summary, the use of amphiphilic PS-*b*-PVP polymeric templates under carefully balanced thermodynamic conditions enables convenient and effective protein immobilization on surfaces with two-dimensional spatial control on the nanometer scale. We have demonstrated that the structural variety and chemical heterogeneity of PS-*b*-PVP template surfaces can be successfully exploited to enable spontaneous formation of self-assembled, hexagonally ordered protein arrays. These protein arrays were rapidly created over a large area on the substrate without the use of external fields. Protein molecules self-assembled exclusively to the PS domains with a nanoscale periodicity. More importantly, protein molecules on the PS-*b*-PVP templates maintained their natural conformation and activity for several months. Our methods involving amphiphilic diblock copolymers to create highly periodic, high-density, surface-bound protein patterns also have the unique capability of controlling the exact repeat spacings of protein nanoarrays two-dimensionally by tuning the size of the underlying PS-*b*-PVP micellar templates. This additional advantage makes our platforms highly suitable as functional sensor substrates or protein arrays which demand precise spatial arrangements of protein molecules in multiple directions. Therefore, our novel two-dimensional protein assembly method will be greatly beneficial for high-throughput proteomic assays and multiplexed biosensing applications.

Acknowledgment. J.H. acknowledges partial support of this work by the Materials Research Institute and the Huck Institutes of the Life Sciences at The Pennsylvania State University.

Supporting Information Available: Additional protein activity measurements were performed on PS-*b*-PVP micellar templates and measured with a confocal fluorescence microscope. The fluorescent images are provided. This material is available free of charge via the Internet at http://pubs.acs.org.

References and Notes

(1) Bieri, C.; Ernst, O. P.; Heyse, S.; Hofmann, K. P.; Vogel, H. *Nat. Biotechnol.* **1999**, *17* (11), 1105−1108.
(2) Ekins, R.; Chu, F. *J. Int. Fed. Clin. Chem.* **1997**, *9* (3), 100−109.
(3) Emili, A. Q.; Cagney, G. *Nat. Biotechnol.* **2000**, *18*, 393−397.
(4) Huang, R. P.; Huang, R.; Fan, Y.; Lin, Y. *Anal. Biochem.* **2001**, *294*, 55−62.
(5) Jenison, R.; La, H.; Haeberli, A.; Ostroff, R.; Polisky, B. *Clin. Chem.* **2001**, *47*, 1894−1900.
(6) Knezevic, V.; Leethanakul, C.; Bichsel, V. E.; Worth, J. M.; Prabhu, V. V.; Gutkind, J. S.; Liotta, L. A.; Munson, P. J.; Petricoin, E. F.; Krizman, D. B. *Proteomics* **2001**, *1*, 1271−1278.
(7) MacBeath, G.; Schreiber, S. L. *Science* **2000**, *289*, 1760−1763.
(8) MacBeath, G. *Nat. Genet.* **2002**, *32*, 526−532.
(9) Madoz-Gurpide, J.; Wang, H.; Misek, D. E.; Brichory, F.; Hanash, S. M. *Proteomics* **2001**, *1*, 1279−1287.
(10) Mazzola, L. T.; Fodor, S. P. *Biophys. J.* **1995**, *68* (5), 1653−1660.
(11) Moody, M. D.; Van Arsdell, S. W.; Murphy, K. P.; Orencole, S. F.; Burns, C. *Biotechniques* **2001**, *31*, 186−194.
(12) Rowe, C. A.; Tender, L. M.; Feldstein, M. J.; Golden, J. P.; Scruggs, S. B.; MacCraith, B. D.; Cras, J. J.; Ligler, F. S. *Anal. Chem.* **1999**, *71* (17), 3846−3852.
(13) Schweitzer, B.; Roberts, S.; Grimwade, B.; Shao, W.; Wang, M.; Fu, Q.; Shu, Q.; Laroche, I.; Zhou, Z.; Tchernev, V. T.; Christiansen, J.; Velleca, M.; Kingsmore, S. F. *Nat. Biotechnol.* **2002**, *20*, 359−365.
(14) Silzel, J. W.; Cercek, B.; Dodson, C.; Tsay, T.; Obremski, R. J. *Clin. Chem.* **1998**, *44* (9), 2036−2043.
(15) Winssinger, N.; Ficarro, S.; Schultz, P. G.; Harris, J. L. *Proc. Natl. Acad. Sci. U.S.A.* **2002**, *99* (17), 11139−11144.
(16) Mendoza, L. G.; McQuary, P.; Mongan, A.; Gangadharan, R.; Brignac, S.; Eggers, M. *Biotechniques* **1999**, *27* (4), 778.
(17) Joos, T. O.; Schrenk, M.; Hopfl, P.; Kroger, K.; Chowdhury, U.; Stoll, D.; Schorner, D.; Durr, M.; Herick, K.; Rupp, S.; Sohn, K.; Hammerle, H. *Electrophoresis* **2000**, *21* (13), 2641−2650.
(18) Kane, R. S.; Takayama, S.; Ostuni, E.; Ingber, D. E.; Whitesides, G. M. *Biomaterials* **1999**, *20* (23−24), 2363−2376.
(19) Brooks, S. A.; Dontha, N.; Davis, C. B.; Stuart, J. K.; O'Neill, G.; Kuhr, W. G. *Anal. Chem.* **2000**, *72* (14), 3253−3259.
(20) Mooney, J. F.; Hunt, A. J.; McIntosh, J. R.; Liberko, C. A.; Walba, D. M.; Rogers, C. T. *Proc. Natl. Acad. Sci. U.S.A.* **1996**, *93* (22), 12287−12291.
(21) Kenseth, J. R.; Harnisch, J. A.; Jones, V. W.; Porter, M. D. *Langmuir* **2001**, *17* (13), 4105−4112.
(22) Wadu-Mesthrige, K.; Xu, S.; Amro, N. A.; Liu, G. Y. *Langmuir* **1999**, *15* (25), 8580−8583.
(23) Lee, K. B.; Park, S. J.; Mirkin, C. A.; Smith, J. C.; Mrksich, M. *Science* **2002**, *295*, (5560), 1702−1705.
(24) Lee, K. B.; Lim, J. H.; Mirkin, C. A. *J. Am. Chem. Soc.* **2003**, *125* (19), 5588−5589.
(25) Bergman, A. A.; Buijs, J.; Herbig, J.; Mathes, D. T.; Demarest, J. J.; Wilson, C. D.; Reimann, C. T.; Baragiola, R. A.; Hu, R.; Oscarsson, S. O. *Langmuir* **1998**, *14* (24), 6785−6788.
(26) Clemmens, J.; Hess, H.; Lipscomb, R.; Hanein, Y.; Bohringer, K. F.; Matzke, C. M.; Bachand, G. D.; Bunker, B. C.; Vogel, V. *Langmuir* **2003**, *19* (26), 10967−10974.
(27) Delamarche, E.; Bernard, A.; Schmid, H.; Michel, B.; Biebuyck, H. *Science* **1997**, *276* (5313), 779−781.
(28) Chiu, D. T.; Jeon, N. L.; Huang, S.; Kane, R. S.; Wargo, C. J.; Choi, I. S.; Ingber, D. E.; Whitesides, G. M. *Proc. Natl. Acad. Sci. U.S.A.* **2000**, *97* (6), 2408−2413.
(29) Patel, N.; Sanders, G. H. W.; Shakesheff, K. M.; Cannizzaro, S. M.; Davies, M. C.; Langer, R.; Roberts, C. J.; Tendler, S. J. B.; Williams, P. M. *Langmuir* **1999**, *15* (21), 7252−7257.
(30) Kumar, N.; Hahm, J. *Langmuir* **2005**, *21*, 6652−6655.
(31) Choucair, A.; Eisenberg, A. *Eur. Phys. J. E* **2003**, *10*, 37−44.
(32) Choucair, A.; Lavigueur, C.; Eisenberg, A. *Langmuir* **2004**, *20* (10), 3894−3900.
(33) Sidorov, S. N.; Bronstein, L. M.; Kabachii, Y. A.; Valetsky, P. M.; Soo, P. L.; Maysinger, D.; Eisenberg, A. *Langmuir* **2004**, *20* (9), 3543−3550.
(34) Zhang, L.; Yu, K.; Eisenberg, A. *Science* **1996**, *272* (5269), 1777−1779.
(35) Park, C.; Yoon, J.; Thomas, E. L. *Polymer* **2003**, *44* (22), 6725−6760.
(36) Yun, S.; Sohn, B.; Jung, J. C.; Zin, W.; Ree, M.; Park, J. W. *Nanotechnology* **2006**, *17*, 450−454.
(37) Hamley, I. W. *Nanotechnology* **2003**, *14*, R39−R54.

(38) Li, X.; Lau, K. H. A.; Kim, D. H.; Knoll, W. *Langmuir* **2005**, *21* (11), 5212−5217.
(39) Spatz, J. P.; Mössmer, S.; Hartmann, C.; Möller, M. *Langmuir* **2000**, *16* (2), 407−415.
(40) Boontongkong, Y.; Cohen, R. E. *Macromolecules* **2002**, *35* (9), 3647−3652.
(41) Kästle, G.; Boyen, H.-G.; Weigl, F.; Lengl, G.; Herzog, T.; Ziemann, P.; Riethmüller, S.; Mayer, O.; Hartmann, C.; Spatz, J. P.; Möller, M.; Ozawa, M.; Banhart, F.; Garnier, M. G.; Oelhafen, P. *Adv. Funct. Mater.* **2003**, *13* (11), 853−861.
(42) Boyen, H.-G.; Kästle, G.; Zürn, K.; Herzog, T.; Weigl, F.; Ziemann, P.; Mayer, O.; Jerome, C.; Möller, M.; Spatz, J. P.; Garnier, M. G.; Oelhafen, P. *Adv. Funct. Mater.* **2003**, *13* (5), 359−364.
(43) Kwon, G. S.; Kataoka, K. *Adv. Drug Delivery Rev.* **1995**, *16* (2), 295−309.
(44) Discher, D. E.; Eisenberg, A. *Science* **2002**, *297* (5583), 967−973.
(45) Hwang, W.; Ham, M.; Sohn, B.; Huh, J.; Kang, Y. S.; Jeong, W.; Myoung, J.; Park, C. *Nanotechnology* **2005**, *16*, 2897−2902.
(46) Chen, L.; Cheung, C. L.; Ashby, P. D.; Lieber, C. M. *Nano Lett.* **2004**, *4* (9), 1725−1731.
(47) Paulo, A. S.; Garcia, R. *Biophys. J.* **2000**, *78* (3), 1599−1605.
(48) Azevedo, A. M.; Martins, V. C.; Prazeres, D. M.; Vojinovic, V.; Cabral, J. M.; Fonseca, L. P. *Biotechnol. Annu. Rev.* **2003**, *9*, 199−247.